

Query-aware Hub Prototype Learning for Few-Shot 3D Point Cloud Semantic Segmentation

Yilin Zhou^{1*}, Lili Wei^{1*}, Zheming Xun^{1*}, Congyan Lang^{1†}, Ziyi Chen¹

¹Key Laboratory of Big Data & Artificial Intelligence in Transportation (Ministry of Education), School of Computer and Information Technology, Beijing Jiaotong University

Abstract

Few-shot 3D point cloud semantic segmentation (FS-3DSeg) aims to segment novel classes with only a few labeled samples. However, existing metric-based prototype learning methods generate prototypes solely from the support set, without considering their relevance to query data. This often results in prototype bias, where prototypes overfit support-specific characteristics and fail to generalize to the query distribution, especially in the presence of distribution shifts, which leads to degraded segmentation performance. To address this issue, we propose a novel Query-aware Hub Prototype (QHP) learning method that explicitly models semantic correlations between support and query sets. Specifically, we propose a Hub Prototype Generation (HPG) module that constructs a bipartite graph connecting query and support points, identifies frequently linked support hubs, and generates query-relevant prototypes that better capture cross-set semantics. To further mitigate the influence of bad hubs and ambiguous prototypes near class boundaries, we introduce a Prototype Distribution Optimization (PDO) module, which employs a purity-reweighted contrastive loss to refine prototype representations by pulling bad hubs and outlier prototypes closer to their corresponding class centers. Extensive experiments on S3DIS and ScanNet demonstrate that QHP achieves substantial performance gains over state-of-the-art methods, effectively narrowing the semantic gap between prototypes and query sets in FS-3DSeg.

Introduction

Point cloud semantic segmentation assigns semantic labels to each point in a 3D point cloud and is essential for applications like autonomous driving and robotics. Although fully supervised methods (Qi et al. 2017b; Lin, Huang, and Wang 2020; Qian et al. 2022) have made significant progress, they rely heavily on costly manual annotations and struggle to generalize to novel classes. To address these challenges, few-shot 3D point cloud segmentation (FS-3DSeg) has gained increasing attention, aiming to learn generalizable models from abundant base class data and adapt the model to novel classes with only a few labeled point clouds.

Recent FS-3DSeg methods typically adopt metric-based prototype learning frameworks, where prototypes are derived from a few labeled support point clouds, and the unlabeled query set is segmented by measuring similarity between query points and these prototypes. As illustrated in Figure 1 (a)(b), these methods can be broadly categorized into two groups: single-prototype approaches (Mao et al. 2022; He et al. 2023; Liu et al. 2024), which generate global class prototypes via masked average pooling, and multi-prototype methods (Zhao, Chua, and Lee 2021; An et al. 2024), which enhance prototype diversity through strategies like Farthest Point Sampling (FPS) and local clustering. Ideally, prototypes should serve as semantic bridges between support and query sets, requiring strong alignment with query semantics. However, existing methods generate prototypes solely from the support set, emphasizing internal representativeness or diversity while ignoring semantic relevance to the query. This often causes prototype bias, especially under distribution shifts between support and query

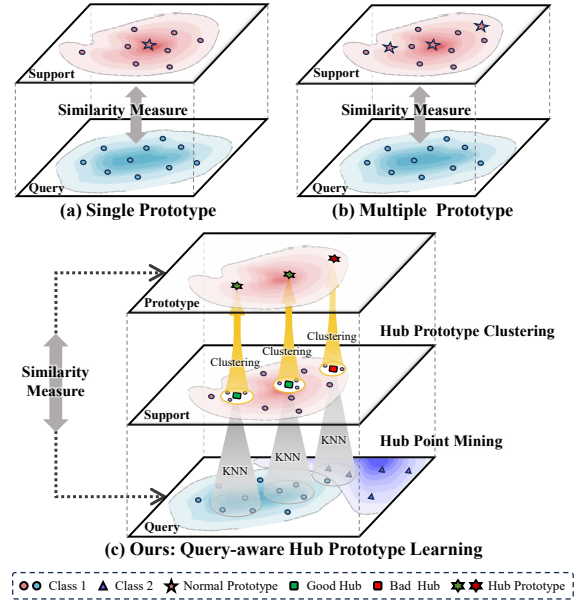


Figure 1: Few-shot 3D point cloud semantic segmentation approaches. (a)(b) Previous prototype learning methods generate prototypes solely based on support points. (c) We propose a Query-aware Hub Prototype Learning method that generates prototypes more closely related to query points.

*These authors contributed equally.

†Corresponding author.

sets. For example, intra-class variations (e.g., square vs. round tables) may share limited similarity, causing prototypes to overfit support-specific traits and poorly represent diverse queries. Moreover, uniform sampling strategies like FPS often introduce redundant or query-irrelevant prototypes, further compromising segmentation accuracy. To address these challenges, it is essential to develop a query-aware prototype generation mechanism to narrow the semantic gap between prototypes and the query set and improve segmentation performance.

Realizing the above issues, we propose a **Query-aware Hub Prototype (QHP)** learning method, as depicted in Figure 1 (c). Hubs (Radovanović, Nanopoulos, and Ivanović 2009) refer to data points that frequently appear among the nearest neighbors of many other points. Therefore, hubs naturally reflect support-query semantic correlation and are well-suited as prototypes. In recent few-shot image classification studies, some methods (Fei et al. 2021; Trosten et al. 2023; Tang et al. 2025) regard hubs as a nightmare and seek to avoid them, worrying that when a support point is a hub, many query points may be retrieved regardless of their true classes. However, we argue that: **(1) Not all hubs are harmful.** Hubs that emerge within the same class (*i.e.*, good hubs) can capture accurate support-query relationships and serve as effective query-aware prototypes, which helps mitigate prototype bias. **(2) The harmful impact of bad hubs is limited in FS-3DSeg.** Since each support sample contains numerous points and provides richer point-level supervision, each query point’s segmentation can be determined by multiple support-query matches, reducing the risk of being misled by any single bad hub. Therefore, instead of suppressing hubs, we leverage them to bridge the semantic gap between support and query, and propose to learn query-aware hub prototypes. Notably, to further mitigate the influence of bad hubs, we optimize their distributions by pulling those near class boundaries closer to corresponding class centers.

The proposed QHP approach introduces two key components: the **Hub Prototype Generation (HPG)** module and the **Prototype Distribution Optimization (PDO)** module. Specifically, HPG explicitly models semantic correlations between support and query sets to learn query-relevant hub prototypes. It constructs a bipartite graph connecting query and support points, identifies support hubs with high linking frequency, and performs local clustering around each hub to generate query-relevant prototypes that better capture cross-set semantics. Query segmentation can be conducted by measuring similarities between query points and these hub prototypes. To further mitigate the influence of bad hubs and ambiguous prototypes near class boundaries, we propose a PDO module during training. PDO constructs a global association graph to identify bad hubs, and adopts a purity-reweighted contrastive loss to pull bad hubs and outlier prototypes toward their corresponding class centers. By jointly leveraging the HPG and PDO modules, our QHP facilitates more query-relevant and discriminative prototype learning, effectively narrowing the semantic gap between prototypes and query sets and yielding improved performance in the FS-3DSeg task.

Our main contributions can be summarized as follows:

- We propose a novel Query-aware Hub Prototype (QHP) Learning method for FS-3DSeg, which explicitly models semantic correlations between support and query sets to generate query-relevant prototypes, addressing prototype bias and narrowing the semantic gap.
- We propose a Hub Prototype Generation (HPG) module to identify support hubs and generate query-relevant hub prototypes that better capture cross-set semantics.
- We design a Prototype Distribution Optimization (PDO) module, optimizing the distributions of bad hubs and outlier prototypes via a purity-reweighted contrastive loss.
- Extensive experiments on S3DIS and ScanNet demonstrate that QHP achieves state-of-the-art performance.

Related Work

3D Point Cloud Semantic Segmentation

Recent 3D point cloud segmentation methods can be broadly categorized into MLP-based (*e.g.*, PointNet (Qi et al. 2017a) and RandLA-Net (Hu et al. 2020)), convolution-based (*e.g.*, PointCNN (Li et al. 2018), KPConv (Thomas et al. 2019), and RandLA-Net (Hu et al. 2020)), and Transformer-based approaches such as Point Transformer (Zhao et al. 2021) and Point Transformer V2 (Wu et al. 2022). Although these methods demonstrate strong performance through local feature aggregation or self-attention mechanisms, they typically require expensive, large-scale annotations and struggle to generalize to novel classes unseen during training.

Few-shot 3D Point Cloud Segmentation

Recent FS-3DSeg methods primarily adopt the prototype-based paradigm built upon metric learning. These methods can be broadly categorized into single-prototype and multi-prototype approaches. Single-prototype methods summarize each class using a single representative prototype from the support set. For instance, ProtoNet defines the prototype as the class-wise mean of support features. To mitigate distribution shifts between support and query sets, 2CBR (Zhu et al. 2023) explicitly models such biases, and DPA (Liu et al. 2024) employs query-guided attention to generate task-adaptive prototypes. However, these methods lack prototype diversity and are unsuitable for handling complex data. To capture intra-class variations, multi-prototype approaches generate multiple prototypes per class. AttMPTI (Zhao, Chua, and Lee 2021) employs farthest point sampling (FPS) to extract diverse local prototypes. Stratified Transformer (Lai et al. 2022) combines hierarchical sampling with cross-window self-attention. COSeg (An et al. 2024) maintains a momentum-updated pool of base class prototypes. Despite these advances, most methods rely solely on support data to generate prototypes, yielding prototypes biased toward support distribution and poorly aligned with queries, thus limiting generalization to novel classes.

The Hubness Phenomenon and Hubs

Hubness (Radovanovic, Nanopoulos, and Ivanovic 2010; Radovanović, Nanopoulos, and Ivanović 2009) describes the tendency of certain points, called *hubs*, to appear frequently

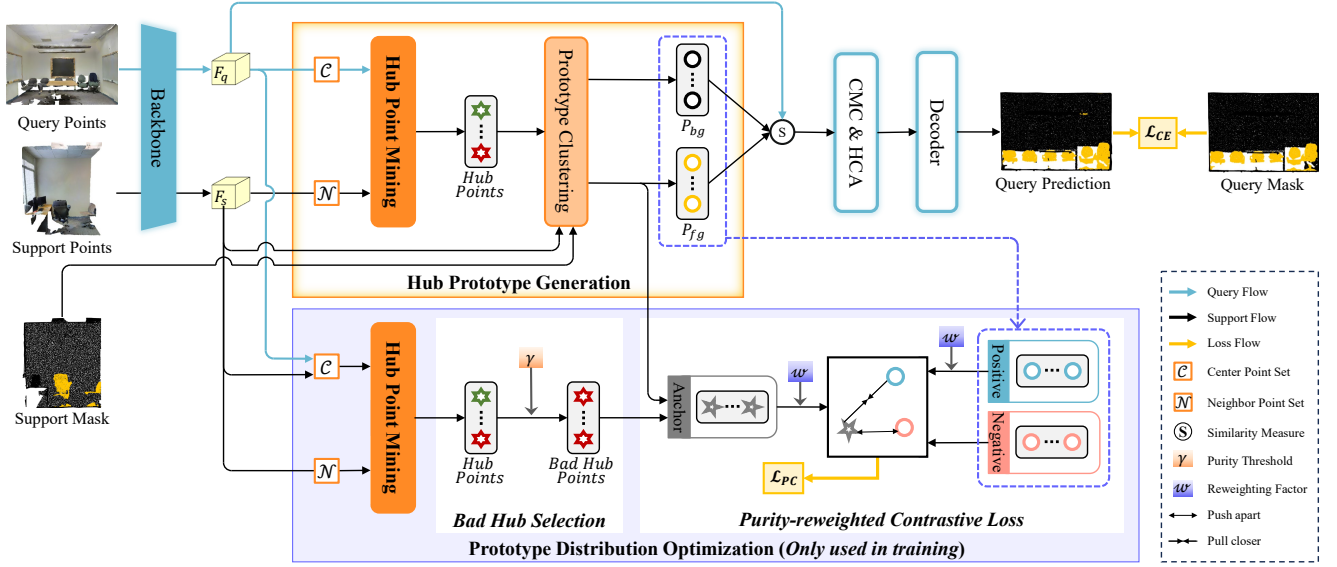


Figure 2: The framework of our Query-aware Hub Prototype Learning method. Initially, we design an HPG module to select support hubs and generate query-relevant hub prototypes. Moreover, during training, a PDO module is integrated to optimize the distribution of bad hubs and outlier prototypes. For clarity, we present the model under the 1-way 1-shot setting.

in nearest-neighbor lists. It has been studied in areas like multi-view clustering (Xu et al. 2025) and cross-modal retrieval (Bogolin et al. 2022; Wang, Jian, and Xue 2023). In few-/zero-shot classification tasks, prior works (Dinu and Baroni 2015; Xiao, Madapana, and Wachs 2021; Cheraghian et al. 2019; Trosten et al. 2023) mostly view hubs as harmful, as query points may be misclassified when dominated by support hubs from different classes. In contrast, we argue that good hubs are beneficial and are primary in our scenario. We thus exploit hubs via query-aware hub prototype learning and mitigate bad hub distance optimization to narrow query-support gaps.

Method

Problem Formulation and Overview

Problem Formulation. FS-3Dseg aims to predict per-point semantic labels for query point clouds using a few labeled support samples. Episodic learning (Zhao, Chua, and Lee 2021) is typically employed to simulate the few-shot learning process, where each C -way K -shot episode includes a support set $S = \{(I_s^{c,k}, M_s^{c,k})_{k=1}^K\}_{c=1}^C$ and a query set $Q = \{(I_q^l, M_q^l)\}_{l=1}^L$. Each point cloud $I_s^{c,k}, I_q^l \in \mathbb{R}^{T \times (3+f_0)}$ contains T points, each represented by 3D coordinates and auxiliary features (e.g., RGB). $M_s^{c,k} \in \{0, 1\}^T$ denotes the binary ground truth (GT) mask indicating whether each point in $I_s^{c,k}$ belongs to class c , while M_q^l denotes the GT labels for the query point cloud I_q^l . During inference, the goal is to predict the query labels \hat{M}_q for the query points in I_q under the guidance of the support set S .

Overview. Figure 2 illustrates the architecture of the proposed QHP framework, comprising two key components: a Hub Prototype Generation (HPG) module and a Pro-

totype Distribution Optimization (PDO) module. We first use a shared backbone Φ to extract point-wise features from the support and query point clouds: $F_s = \Phi(I_s) \in \mathbb{R}^{C \times K \times T \times D}$ and $F_q = \Phi(I_q) \in \mathbb{R}^{L \times T \times D}$, where D is the channel dimension. In the HPG module, a Hub Point Mining (HPM) module identifies hub points from S , which are used to generate hub prototypes P via local clustering. These prototypes are matched with query features F_q through similarity measures, and further refined via the CMC and HCA modules (An et al. 2024) to yield query predictions \hat{M}_q . To mitigate the influence of bad hubs and ambiguous prototypes, our PDO module identifies bad hubs by thresholding their purity and applies a Purity-reweighted Contrastive (PC) loss to promote intra-class compactness. During training, our model is jointly optimized by a cross-entropy (CE) loss and the proposed PC loss.

Subsequently, we provide a detailed description of the HPG module, PDO module and each loss as below.

Hub Prototype Generation

To mitigate prototype bias, we propose an HPG module. It first identifies frequently occurring support hubs via a Hub Point Mining (HPM) module, then generates query-relevant hub prototypes through Hub Prototype Clustering.

Hub Point Mining. HPM identifies hub points through three sequential steps, as illustrated in Figure 3(a)–(c).

Step 1: k -Nearest Neighbor Mining. Given a center point set \mathcal{C} and a neighbor point set \mathcal{N} , a bipartite graph is constructed by connecting each center point $c \in \mathcal{C}$ to its k -nearest (k NN) neighbors in \mathcal{N} via cosine similarity measure. The k -nearest neighbors of c are formulated as $k\text{NN}(c, \mathcal{N})$.

Step 2: Hubness Score Statistic. The hubness score $s(n)$ quantifies how frequently a point $n \in \mathcal{N}$ is selected as

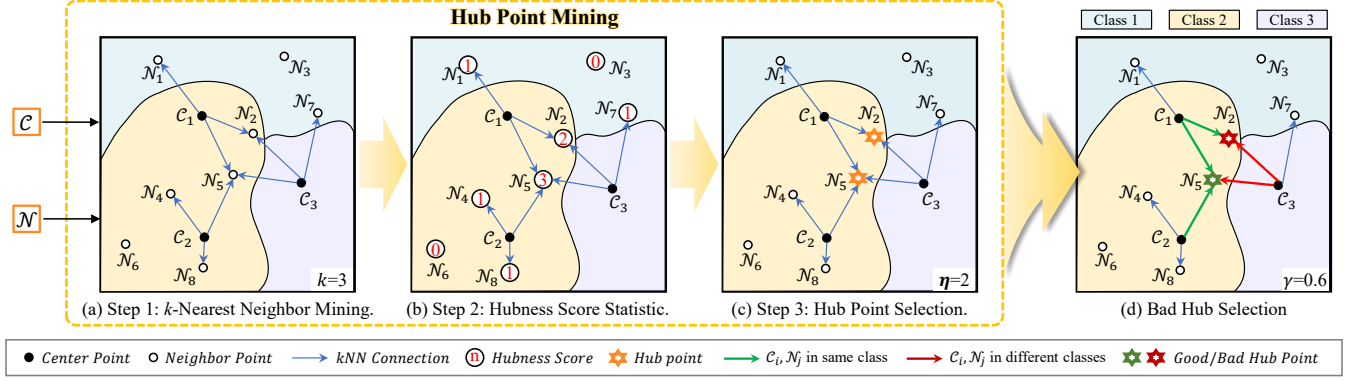


Figure 3: Illustration of Hub Point Mining and Bad Hub Selection modules. We give an example under hyperparameters $k = 3$, $\eta = 2$, and $\gamma = 0.6$. (a)–(c) Hub Point Mining: initially, using center points $\{C_1, C_2, C_3\}$ and neighbor points $\{N_1, \dots, N_8\}$ as input, a k NN graph is constructed with $k = 3$. After calculating hubness scores, the top $\eta = 2$ points with the highest hubness scores are selected as hubs. (d) Bad Hub Selection: Hubs with purity below the threshold $\gamma = 0.6$ are selected as bad hubs.

neighbors by all center points in \mathcal{C} , defined as:

$$s(n) = \sum_{c \in \mathcal{C}} \mathbb{1}(n \in k\text{NN}(c, \mathcal{N})) + \varepsilon, \quad (1)$$

where $\mathbb{1}(\cdot)$ denotes the Iverson bracket indicator function, returning 1 if the condition holds and 0 otherwise. A small positive constant ε is added to avoid zero scores caused by potential outliers, ensuring $s(n) > 0$ for all n . The collective hubness scores for all points in \mathcal{N} are denoted as $s(\mathcal{N})$.

Step 3: Hub Point Selection. To identify nodes most frequently regarded as neighbors by center points, we select a subset $\mathcal{H} \subseteq \mathcal{N}$ consisting of the top- η neighbor points with the highest hubness scores, defined as:

$$\mathcal{H} = \{n \in \mathcal{N} \mid s(n) \in \text{Top-}\eta(s(\mathcal{N}))\}. \quad (2)$$

Hub Prototype Clustering. Before prototype clustering, we treat points in the query set Q and support set S as input node sets \mathcal{C} and \mathcal{N} of the HPM module, and select Top- η hub points for each class to construct hub point set \mathcal{H} .

A prototype set $P = P_{fg} \cup P_{bg}$, where P_{fg} and P_{bg} denote foreground/background prototypes, is generated by conducting point-to-seed clustering (Zhao, Chua, and Lee 2021) on support features localized around each hub point, defined as:

$$\begin{aligned} P_{fg} &= \mathcal{F}_{clus}(F_s \odot M_s, \mathcal{H}_{fg}), \mathcal{H}_{fg} = \mathcal{H} \odot M_s, \\ P_{bg} &= \mathcal{F}_{clus}(F_s \odot \neg M_s, \mathcal{H}_{bg}), \mathcal{H}_{bg} = \mathcal{H} \odot \neg M_s, \end{aligned} \quad (3)$$

where \odot denotes the Hadamard product; M_s and $\neg M_s$ are the GT mask and its inverse for support set; \mathcal{H}_{fg} and \mathcal{H}_{bg} are foreground/background hub point subsets; and \mathcal{F}_{clus} denotes the clustering operation. After that, we obtain η prototypes per class, yielding a total of $(C + 1) \cdot \eta$ prototypes.

Notably, although support hubs \mathcal{H} originate from S , they are geometrically closer to points in Q as they retain only those support points that best match the query distribution. Consequently, the derived hub prototypes are more aligned with Q in the metric space, facilitating improved prototype-query matching and enhanced segmentation performance.

Prototype Distribution Optimization

In the PDO module, we select potential bad hubs, and then adopt a Purity-reweighted Contrastive (PC) loss to suppress these bad hubs and optimize the prototype distribution.

Bad Hub Selection. To select bad hubs, we construct a global association graph via k NN algorithm, where we merge points from Q and S to form the center point set, treat S as neighbor point set \mathcal{N} , and then utilize the HPM module to identify hub points \mathcal{H} from support set S .

After that, we focus on identifying all potential bad hubs within \mathcal{H} , i.e., those exhibiting stronger connections to center points belonging to different classes, as illustrated in Figure 3(d). This process contains three steps:

First, we compute the number of times each hub h is connected to center points of the same class, denoted as $t(h)$:

$$t(h) = \sum_{c \in \mathcal{C}} \mathbb{1}(h \in k\text{NN}(c, \mathcal{N})) \cdot \mathbb{1}(M_h = M_c), \quad (4)$$

where M_c, M_h are class labels of c and h , respectively.

Next, a purity $\mathcal{P}(h)$ is defined to represent the proportion of connections to center points of the same class, given by:

$$\mathcal{P}(h) = t(h)/s(h). \quad (5)$$

Finally, the bad hub point set \mathcal{BH} is filtered out using a purity threshold $\gamma \in (0, 1)$, formulated as:

$$\mathcal{BH} = \{h \in \mathcal{H} \mid \mathcal{P}(h) < \gamma\}. \quad (6)$$

Purity-reweighted Contrastive Loss. To further eliminate the influence of bad hubs and outlier prototypes, we aim to pull them back to their cluster centers. A typical solution is contrastive learning (Wang and Liu 2021), which has been widely adopted in various areas to pull positive pairs closer and push negative pairs apart. Despite these successes, contrastive loss has not been explored in FS-3DSeg. However, directly applying standard contrastive loss to bad hub anchors is suboptimal: low-purity anchors, which have high similarity to samples from other classes, tend to lie far from their true class centers and are more likely to be confused,

thus requiring stronger guidance to be correctly aligned. To tackle this issue, we propose a Purity-reweighted Contrastive (PC) loss, which dynamically adjusts the attraction strength based on the purity of each anchor sample.

We first introduce a purity reweighting factor $w(a)$ to quantify the strength with which anchor $a \in \mathcal{A} = \{P_{fg} \cup \mathcal{BH}\}$ is pulled toward positive prototypes, formulated as:

$$w(a) = \begin{cases} 1 - \mathcal{P}(a) & \text{if } a \in \mathcal{BH} \\ 1 & \text{otherwise } a \in P_{fg} \end{cases}, \quad (7)$$

where the first line assigns a higher weight ($w(a) \rightarrow 1$) inversely proportional to purity for bad hub anchors ($a \in \mathcal{BH}$) with low purity ($\mathcal{P}(a) \rightarrow 0$), strongly pulling them toward class centers; the second line assigns a fixed weight ($w(a) = 1$) for all foreground prototype anchors ($a \in P_{fg}$), ensuring intra-class compactness and inter-class discriminability.

Based on the defined purity reweighting factor $w(a)$, we formulate our purity-reweighted contrastive loss for all anchors \mathcal{A} as follows,

$$\mathcal{L}_{PC} = -\frac{1}{|\mathcal{A}|} \sum_{a \in \mathcal{A}} \log \frac{w(a) \cdot U^+(a)}{w(a) \cdot U^+(a) + U^-(a)}, \quad (8)$$

$$U^{+/-}(a) = \sum_{p \in P^{+/-}(a)} \exp(\text{sim}(a, p)/\tau),$$

where $P^+(a) = \{p \in P \mid M_p = M_a\}$ and $P^-(a) = \{p \in P \mid M_p \neq M_a\}$ are positive set and negative set, respectively; τ is a temperature parameter that controls smoothing; $\text{sim}(a, p)$ is the similarity between a and p .

Total Loss

During training, the proposed model is supervised by two loss functions, *i.e.*, a standard cross-entropy loss \mathcal{L}_{CE} that serves to optimize segmentation results, and the proposed PC loss \mathcal{L}_{PC} to optimize the prototype distributions. Specifically, the cross-entropy loss \mathcal{L}_{CE} is defined as:

$$\mathcal{L}_{CE} = -\frac{1}{L} \sum_{l=1}^L M_q^l \log(\hat{M}_q^l), \quad (9)$$

where M_q^l and \hat{M}_q^l represent GT mask and the predicted mask for query sample.

The overall loss is a weighted combination of \mathcal{L}_{CE} and \mathcal{L}_{PC} with a balancing weight λ , represented as:

$$\mathcal{L}_{total} = \mathcal{L}_{CE} + \lambda \cdot \mathcal{L}_{PC}. \quad (10)$$

Experiments

Datasets and Implementation Details

Datasets. We conducted experiments on the S3DIS and ScanNet datasets. The S3DIS dataset (Armeni et al. 2016) comprises five large-scale indoor areas across three buildings, annotated with 12 semantic classes for segmentation tasks. The ScanNet dataset (Dai et al. 2017) contains 1,513 point cloud scans from 707 indoor scenes, covering 20 semantic categories. Compared to S3DIS, ScanNet features more irregular point clouds, rendering segmentation more

challenging. Data preprocessing follows (An et al. 2024): each room is divided into $1\text{m} \times 1\text{m}$ blocks, input points are grid-sampled at 0.02m intervals, and after voxelization, 20,480 points are selected to standardize the input size.

Training. We adopt data augmentation and pre-training protocols following COSeg (An et al. 2024), with the backbone pre-trained on each fold for 100 epochs. Meta-training is performed over 40,000 episodes using the AdamW optimizer, with a learning rate of 5×10^{-5} and weight decay of 0.01. For testing, we sample 1,000 episodes per class in 1-way settings and 100 episodes per combination in 2-way settings to ensure stable evaluations. We use 100 prototypes per class ($\eta = 100$). In k -shot scenarios where $k > 1$, η/k prototypes are selected from each shot and concatenated to form the final prototypes. All models are implemented in PyTorch and trained on four NVIDIA RTX A4000 GPUs.

Parameters. In both the HPG and PDO modules, the number of neighbors for hub point mining is set to $k = 5$. In the HPG module, the number of hub points/prototypes per class is set to $\eta = 100$. In the PDO module, the bad hub purity threshold is set to $\gamma = 0.6$ in (Eq. 6). In the total loss function (Eq. 10), the balance weight for \mathcal{L}_{PC} is set to $\lambda = 0.1$.

Comparison Results

Comparison with Previous Methods. We compare our QHP with prior works including AttMPTI (Zhao, Chua, and Lee 2021), QGE (Ning et al. 2023), QGPA (He et al. 2023), and COSeg (An et al. 2024) on S3DIS and ScanNet datasets.

- **S3DIS.** Table 1 shows that our QHP consistently outperforms prior approaches across all settings. Specifically, compared to the baseline method COSeg, QHP achieves performance gains of 2.82% and 2.36% in the 1-way 1-shot and 1-way 5-shot settings, and enhancements of 1.25% and 1.64% in the 2-way settings. These gains can be attributed to the hub prototypes generated by our method. Unlike COSeg, which relies on FPS-based prototype generation that may produce redundant or irrelevant prototypes, our HPG module effectively identifies hub points to generate query-relevant prototypes, leading to more accurate segmentation outcomes. Additionally, optimizing prototype distributions further contributes to the superior performance of our model. When compared to query-guided methods such as QGE and QGPA, QHP demonstrates more significant advantages in the 1-way tasks, with improvements of 9.14% and 2.46%, respectively. This highlights the superiority of our method in enhancing the discriminability of prototypes.

- **ScanNet.** Table 2 shows that QHP outperforms all prior methods across all settings, further validating the effectiveness and applicability of our approach. Notably, in the 1-way 5-shot task, QHP achieves a mIoU of 47.45% and outperforms COSeg by 1.19%, which highlights QHP’s adaptability to the complex and diverse ScanNet dataset. We note that our performance gains are more pronounced in 5-shot than 1-shot settings: with more support samples available, QHP can mine important hub points from a larger pool of support points to generate query-relevant prototypes, thus capturing class-specific features more effectively. However, improvements on ScanNet are less substantial than S3DIS, as

Methods	1-way 1-shot			1-way 5-shot			2-way 1-shot			2-way 5-shot		
	S^0	S^1	mean	S^0	S^1	mean	S^0	S^1	mean	S^0	S^1	mean
AttMPTI	36.32	38.36	37.34	46.71	42.70	44.71	31.09	29.62	30.36	39.53	32.62	36.08
QGE	41.69	39.09	40.39	50.59	46.41	48.50	33.45	30.95	32.20	40.53	36.13	38.33
QGPA	35.50	35.83	35.67	38.07	39.70	38.89	25.52	26.26	25.89	30.22	32.41	31.31
COSeg	45.93	47.48	46.71	48.47	48.72	48.60	37.17	37.03	37.10	42.27	38.38	40.33
QHP (ours)	50.33	48.73	49.53	52.27	49.64	50.96	38.86	37.84	38.35	43.90	40.04	41.97

Table 1: Comparisons of mIoU (%) performance between our method and previous FS-3DSeg approaches on the **S3DIS** dataset. The best results are shown in **bold**.

Methods	1-way 1-shot			1-way 5-shot			2-way 1-shot			2-way 5-shot		
	S^0	S^1	mean	S^0	S^1	mean	S^0	S^1	mean	S^0	S^1	mean
AttMPTI	34.03	30.97	32.50	39.09	37.15	38.12	25.99	23.88	24.94	30.41	27.35	28.88
QGE	37.38	33.02	35.20	45.08	41.89	43.49	26.85	25.17	26.01	28.35	31.49	29.92
QGPA	34.57	33.37	33.97	41.22	38.65	39.94	21.86	21.47	21.67	30.67	27.69	29.18
COSeg	40.57	41.94	41.26	49.43	43.57	46.50	28.06	28.92	28.49	35.49	33.39	34.49
QHP (ours)	40.70	42.92	41.81	50.10	44.80	47.45	28.45	29.07	28.76	36.11	34.30	35.21

Table 2: Comparisons of mIoU (%) performance between our method and previous FS-3DSeg approaches on the **ScanNet** dataset. The best results are shown in **bold**.

Baseline	HPG	PDO	mIoU (%)
✓			45.93
✓	✓		47.37
✓	✓	✓	50.33

Table 3: Ablation study of key components in QHP method.

the dataset’s higher complexity and inter-class overlap pose greater challenges for distinguishing similar categories.

Qualitative Results. In Figure 4, we compare the results from our QHP (6th column) with those from COSeg (5th column). QHP improves object boundaries and category shapes, especially for column contours (blue, 2nd row), capturing finer details and reducing redundancy. The PDO module excels in the chair class (yellow, 1st row), resolving boundary ambiguities for more precise segmentation. Overall, QHP delivers cleaner, more accurate results with improved boundary delineation and reduced redundancy.

Ablation Study

We present an ablation study on the S3DIS dataset under 1-way 1-shot S^0 setting to validate the effectiveness of HPG and PDO modules, as well as hyperparameter settings.

Effects of Core Components. Using COSeg as the baseline, we conduct experiments to evaluate the effectiveness of the two core components, *i.e.*, the HPG and PDO modules. As shown in Table 3, incorporating the HPG module improves the mIoU from 45.93% to 47.37% (+1.44%), while the addition of the PDO module further increases the mIoU to 50.33% (+2.96%), showing that the joint use of HPG

Hub Prototype Ratio	0%	30%	50%	80%	100%
mIoU (%)	45.93	42.93	42.32	45.47	47.37

Table 4: Analyze the ratio of hub prototypes in HPG.

and PDO significantly enhances the query relevance and discriminability of the prototypes, thereby leading to substantial performance gains.

Effects of Hub Prototypes from HPG. Without using the PDO module, we fix the number of prototypes to 100 per class and mix FPS-based prototypes with our hub prototypes in varying ratios. As the hub prototype ratio increases from 0% (*i.e.*, baseline COSeg) to 50%, performance slightly drops, likely because prototype class diversity is reduced while the query relevance of prototypes remains limited, causing suboptimal performance. Beyond 50%, performance steadily improves, peaking at 100%, demonstrating that hub prototypes better capture support-query semantic correlation and provide more discriminative representations, significantly enhancing segmentation.

Impact of Parameters k and η in HPG. We analyze the impact of the number of neighborhoods k in Eq. 1 and the number of hub points η in Eq. 2, as shown in Figure 5(a). The best performance is achieved when $k = 12$ and $\eta = 50$, followed by $k = 5$ and $\eta = 100$. For fair comparison with other multi-prototype methods with 100 prototypes, we select the setting $k = 5$ and $\eta = 100$.

Impact of Parameters k and γ in PDO. We analyze the impact of the number of neighborhood k and purity threshold

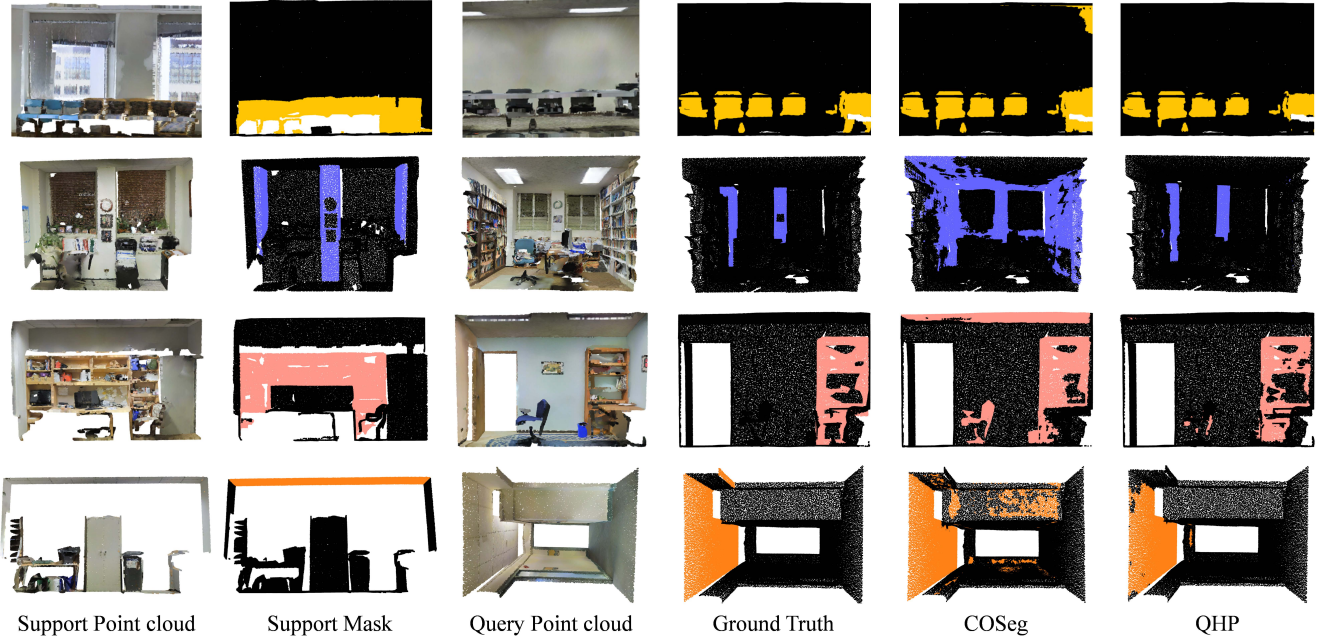


Figure 4: Qualitative comparisons between our proposed model QHP and COSeg. Each row, from top to bottom, represents the 1-way 1-shot task with the target category as chair (yellow), column (blue), bookcase (pink), and ceiling (orange), respectively.

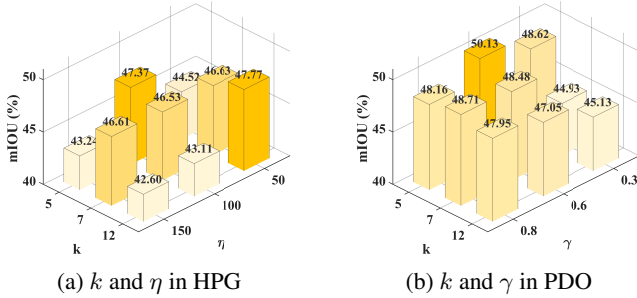


Figure 5: Parameter sensitivity analysis of HPG and PDO.

γ in PDO, as shown in Figure 5(b). The best performance is achieved when $k = 5$ and $\gamma = 0.6$; thus, these parameters are selected in our setup.

Effects of Different Contrastive Losses in PDO. To verify the superiority of our proposed PC loss, we compared the effects of using the PC loss and the standard contrastive loss in the PDO module, as shown in Table 5. Our PC loss yields a 0.51% performance improvement, demonstrating that with the reweighting factor in our PC loss, both outlier prototypes and bad hubs near cluster boundaries are more effectively pulled into their respective class centers. This reduces boundary ambiguity and thus enhances overall performance.

Impact of Coefficient λ in Total Loss. Table 6 illustrates the impact of the weight λ of the PC loss in Eq. 10. An appropriate value of $\lambda = 0.1$ yields the best results, indicating that the model achieves a balance between class boundary distribution and query segmentation. However, continued increases in λ could pull prototypes and hub points too tightly

Different Losses	Contrastive Loss	Our PC Loss
mIoU (%)	49.82	50.33

Table 5: Comparison between PC loss and contrastive loss.

λ	0.9	0.7	0.5	0.3	0.1	0
mIoU (%)	38.28	44.06	45.08	44.10	50.33	47.37

Table 6: Impact of the coefficient λ for \mathcal{L}_{PC} in the total loss.

into clusters, thereby harming model performance.

We also provide more ablation studies in the *Supplemental Material* to present more detailed designs of our model.

Conclusion

We propose a Query-aware Hub Prototype (QHP) framework for few-shot 3D point cloud semantic segmentation, addressing limitations of prior methods relying solely on support prototypes. QHP models semantic correlations between support and query sets to enhance prototype relevance, with two key modules: a Hub Prototype Generation (HPG) module, identifying high-frequency hub points from support to generate query-relevant prototypes; and a Prototype Distribution Optimization (PDO) module, reducing the impact of bad hubs and ambiguous prototypes via purity-reweighted contrastive loss. Experiments on S3DIS and ScanNet show the superiority of the proposed model.

References

- An, Z.; Sun, G.; Liu, Y.; Liu, F.; Wu, Z.; Wang, D.; Van Gool, L.; and Belongie, S. 2024. Rethinking few-shot 3d point cloud semantic segmentation. In *Proceedings of the IEEE/CVF Conference on Computer Vision and Pattern Recognition (CVPR)*, 3996–4006.
- Armeni, I.; Sener, O.; Zamir, A. R.; Jiang, H.; Brilakis, I.; Fischer, M.; and Savarese, S. 2016. 3d semantic parsing of large-scale indoor spaces. In *Proceedings of the IEEE/CVF Conference on Computer Vision and Pattern Recognition (CVPR)*, 1534–1543.
- Bogolin, S.-V.; Croitoru, I.; Jin, H.; Liu, Y.; and Albanie, S. 2022. Cross modal retrieval with querybank normalisation. In *Proceedings of the IEEE/CVF Conference on Computer Vision and Pattern Recognition (CVPR)*, 5184–5195.
- Cheraghian, A.; Rahman, S.; Campbell, D.; and Petersson, L. 2019. Mitigating the Hubness Problem for Zero-Shot Learning of 3D Objects. In *Proceedings of the British Machine Vision Conference (BMVC)*, 41.
- Dai, A.; Chang, A. X.; Savva, M.; Halber, M.; Funkhouser, T.; and Nießner, M. 2017. Scannet: Richly-annotated 3d reconstructions of indoor scenes. In *Proceedings of the IEEE/CVF Conference on Computer Vision and Pattern Recognition (CVPR)*, 5828–5839.
- Dinu, G.; and Baroni, M. 2015. Improving zero-shot learning by mitigating the hubness problem. In *International Conference on Learning Representations (ICLR)*.
- Fei, N.; Gao, Y.; Lu, Z.; and Xiang, T. 2021. Z-Score Normalization, Hubness, and Few-Shot Learning. In *Proceedings of the IEEE/CVF International Conference on Computer Vision (ICCV)*, 142–151.
- He, S.; Jiang, X.; Jiang, W.; and Ding, H. 2023. Prototype Adaption and Projection for Few- and Zero-Shot 3D Point Cloud Semantic Segmentation. *IEEE Transactions on Image Processing (TIP)*, 32: 3199–3211.
- Hu, Q.; Yang, B.; Xie, L.; Rosa, S.; Guo, Y.; Wang, Z.; Trigoni, N.; and Markham, A. 2020. RandLA-Net: Efficient Semantic Segmentation of Large-Scale Point Clouds. In *Proceedings of the IEEE/CVF Conference on Computer Vision and Pattern Recognition (CVPR)*, 11105–11114.
- Lai, X.; Liu, J.; Jiang, L.; Wang, L.; Zhao, H.; Liu, S.; Qi, X.; and Jia, J. 2022. Stratified transformer for 3d point cloud segmentation. In *Proceedings of the IEEE/CVF Conference on Computer Vision and Pattern Recognition (CVPR)*, 8500–8509.
- Li, Y.; Bu, R.; Sun, M.; Wu, W.; Di, X.; and Chen, B. 2018. PointCNN: Convolution On X-Transformed Points. In *Advances in Neural Information Processing Systems (NeurIPS)*, 828–838.
- Lin, Z.-H.; Huang, S.-Y.; and Wang, Y.-C. F. 2020. Convolution in the Cloud: Learning Deformable Kernels in 3D Graph Convolution Networks for Point Cloud Analysis. In *Proceedings of the IEEE/CVF Conference on Computer Vision and Pattern Recognition (CVPR)*, 1797–1806.
- Liu, J.; Yin, W.; Wang, H.; Chen, Y.; Sonke, J.-J.; and Gavves, E. 2024. Dynamic Prototype Adaptation with Distillation for Few-shot Point Cloud Segmentation. In *International Conference on 3D Vision (3DV)*, 810–819.
- Mao, Y.; Guo, Z.; Xiaonan, L.; Yuan, Z.; and Guo, H. 2022. Bidirectional Feature Globalization for Few-shot Semantic Segmentation of 3D Point Cloud Scenes. In *International Conference on 3D Vision (3DV)*, 505–514.
- Ning, Z.; Tian, Z.; Lu, G.; and Pei, W. 2023. Boosting Few-shot 3D Point Cloud Segmentation via Query-Guided Enhancement. In *Proceedings of the ACM International Conference on Multimedia (ACMMM)*, MM ’23, 1895–1904.
- Qi, C. R.; Su, H.; Mo, K.; and Guibas, L. J. 2017a. Pointnet: Deep learning on point sets for 3d classification and segmentation. In *Proceedings of the IEEE/CVF Conference on Computer Vision and Pattern Recognition (CVPR)*, 652–660.
- Qi, C. R.; Yi, L.; Su, H.; and Guibas, L. J. 2017b. Pointnet++: Deep hierarchical feature learning on point sets in a metric space. In *Advances in Neural Information Processing Systems (NeurIPS)*, 5099–5108.
- Qian, G.; Li, Y.; Peng, H.; Mai, J.; Hammoud, H.; Elhoseiny, M.; and Ghanem, B. 2022. Pointnext: Revisiting pointnet++ with improved training and scaling strategies. In *Advances in Neural Information Processing Systems (NeurIPS)*.
- Radovanović, M.; Nanopoulos, A.; and Ivanović, M. 2009. Nearest neighbors in high-dimensional data: The emergence and influence of hubs. In *International conference on machine learning (ICML)*, 865–872.
- Radovanovic, M.; Nanopoulos, A.; and Ivanovic, M. 2010. Hubs in space: Popular nearest neighbors in high-dimensional data. *Journal of Machine Learning Research (JMLR)*, 11(sept): 2487–2531.
- Tang, W.; Pei, H.; Wang, X.; He, Z.; Yu, L.; and Yang, X. 2025. Reducing hubness to improve inductive few-shot learning. *Neurocomputing*, 651: 130879.
- Thomas, H.; Qi, C. R.; Deschaud, J.-E.; Marcotegui, B.; Goulette, F.; and Guibas, L. J. 2019. KPConv: Flexible and Deformable Convolution for Point Clouds. In *Proceedings of the IEEE/CVF International Conference on Computer Vision (ICCV)*, 6410–6419.
- Trosten, D. J.; Chakraborty, R.; Løkse, S.; Wickstrøm, K. K.; Jenssen, R.; and Kampffmeyer, M. C. 2023. Hubs and Hyperspheres: Reducing Hubness and Improving Transductive Few-Shot Learning With Hyperspherical Embeddings. In *Proceedings of the IEEE/CVF Conference on Computer Vision and Pattern Recognition (CVPR)*, 7527–7536.
- Wang, F.; and Liu, H. 2021. Understanding the Behaviour of Contrastive Loss. In *Proceedings of the IEEE/CVF Conference on Computer Vision and Pattern Recognition (CVPR)*, 2495–2504.
- Wang, Y.; Jian, X.; and Xue, B. 2023. Balance Act: Mitigating Hubness in Cross-Modal Retrieval with Query and Gallery Banks. In *Conference on Empirical Methods in Natural Language Processing (EMNLP)*, 10542–10567.

- Wu, X.; Lao, Y.; Jiang, L.; Liu, X.; and Zhao, H. 2022. Point Transformer V2: Grouped Vector Attention and Partition-based Pooling. In *Advances in Neural Information Processing Systems (NeurIPS)*, 33330–33342.
- Xiao, C.; Madapana, N.; and Wachs, J. 2021. One-shot image recognition using prototypical encoders with reduced hubness. In *2019 IEEE Winter Conference on Applications of Computer Vision (WACV)*, 2251–2260.
- Xu, Z.; Liu, H.; Lang, C.; Wang, T.; Li, Y.; and Kampffmeyer, M. C. 2025. A Hubness Perspective on Representation Learning for Graph-Based Multi-View Clustering. In *Proceedings of the IEEE/CVF Conference on Computer Vision and Pattern Recognition (CVPR)*, 15528–15537.
- Zhao, H.; Jiang, L.; Jia, J.; Torr, P. H.; and Koltun, V. 2021. Point Transformer. In *Proceedings of the IEEE/CVF International Conference on Computer Vision (ICCV)*, 16259–16268.
- Zhao, N.; Chua, T.-S.; and Lee, G. H. 2021. Few-shot 3d point cloud semantic segmentation. In *Proceedings of the IEEE/CVF Conference on Computer Vision and Pattern Recognition (CVPR)*, 8873–8882.
- Zhu, G.; Zhou, Y.; Yao, R.; and Zhu, H. 2023. Cross-Class Bias Rectification for Point Cloud Few-Shot Segmentation. *IEEE Transactions on Multimedia (TMM)*, 25: 9175–9188.